

Photoswitchable Fluorescent Crystals Obtained by the Photoreversible Coassembly of a Nucleobase and an Azobenzene Intercalator

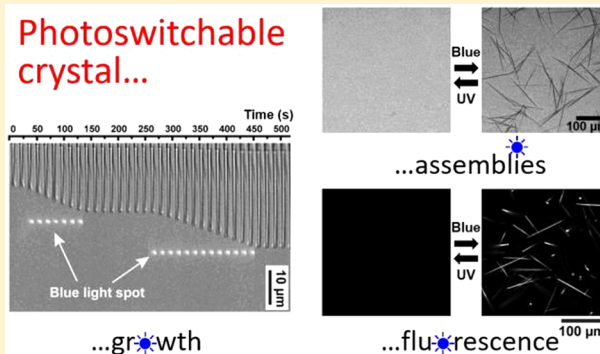
Li Zhou,^{†,§} Pascal Retailleau,[‡] Mathieu Morel,[†] Sergii Rudiuk,[†] and Damien Baigl^{*,†,§}

[†]PASTEUR, Department of Chemistry, Ecole Normale Supérieure, PSL University, Sorbonne Université, CNRS, Paris 75005, France

[‡]Institut de Chimie des Substances Naturelles, CNRS UPR 2301, Université Paris-Sud, Université Paris-Saclay, 1 av. de la Terrasse, Gif-sur-Yvette 91198, France

Supporting Information

ABSTRACT: Self-assembled nucleobases, such as G-quartets or quadruplexes, have numerous applications, but light-responsive structures are limited to small, noncrystalline motifs. In addition, the assembly of the widely exploited azobenzene photochromic compounds can produce fluorescent crystals of extended dimensions but at the prize of sacrificing their photoswitchability. Here, we overcome inherent limitations of self-assembly with a new concept of supramolecular coassembly leading to materials with unprecedented properties. We show that the coassembly of guanosine monophosphate (GMP) with an azobenzene-containing DNA intercalator produces supramolecular crystals arranged through a combination of π – π , electrostatic, and hydrogen-bond interactions. The resulting crystals are 100 μ m long, pH-sensitive, fluorescent, and can be photoreversibly disassembled/reassembled upon UV/blue irradiation. This allows us to perform operations such as dynamic photocontrol of a single-crystal growth, light-gated permeability in membrane-like materials, and photoswitchable fluorescence. We believe this concept critically expands the breadth of multifunctional materials attainable by self-assembly.



INTRODUCTION

Systems with light-switchable functions are appealing for fields ranging from biology to physics and material science.^{1–3} Azobenzene is one of the most attractive photochromes used in such systems because of its robust, rapid, and reversible *E/Z* isomerization that leads to large changes in molecular geometry and polarity.⁴ Applications of azobenzene derivatives in holographic memory storage, optoelectronic devices, optofluidics, molecular machines, responsive materials, energy conversion, and drug design have been widely explored by taking advantage of their robust photoisomerization characteristics.^{5–11} However, this remarkable photoisomerization ability tends to hinder photochromic azobenzene derivatives from exhibiting fluorescence properties. By imparting azobenzene with steric rigidity, bright fluorescence can be achieved, but this is usually done at the price of sacrificing the photoisomerization capability.^{12,13} Realizing a system displaying both azobenzene fluorescence and photoisomerization capability, an interesting combination, for instance, to optically modulate fluorescence, is thus a desirable challenge that has been achieved in a few rare cases. The typical strategy has consisted of controlling with light the aggregation behavior of azobenzene derivatives, which, by exploiting the fluorescence

enhancement effect upon aggregation, led to a variety of light-dependent aggregating systems with optically tunable emission characteristics.^{14–19} These materials were, however, usually morphologically ill-defined and poorly structured. Conversely, well-defined azobenzene crystals with bright fluorescence properties were obtained but did not display any photo-switching characteristics.^{20–22} Finally, light-responsive organized assembly of azobenzenes was reported, but the fluorescence properties were either not documented²³ or modestly affected by light.²⁴ Note that most of the above-mentioned examples were based on the assembly of hydrophobic or amphiphilic compounds in organic solvents. To our knowledge, highly organized azobenzene-based supramolecular structures, such as crystals, with both light-responsive organization and on/off photoswitchable fluorescence have never been realized. Here, we report the first light-responsive azobenzene crystals with photoswitchable fluorescence in water. These crystals were obtained following a new strategy consisting of the coassembly of azobenzene-containing DNA intercalators and nucleobases as noncovalently interacting

Received: March 20, 2019

Published: May 22, 2019

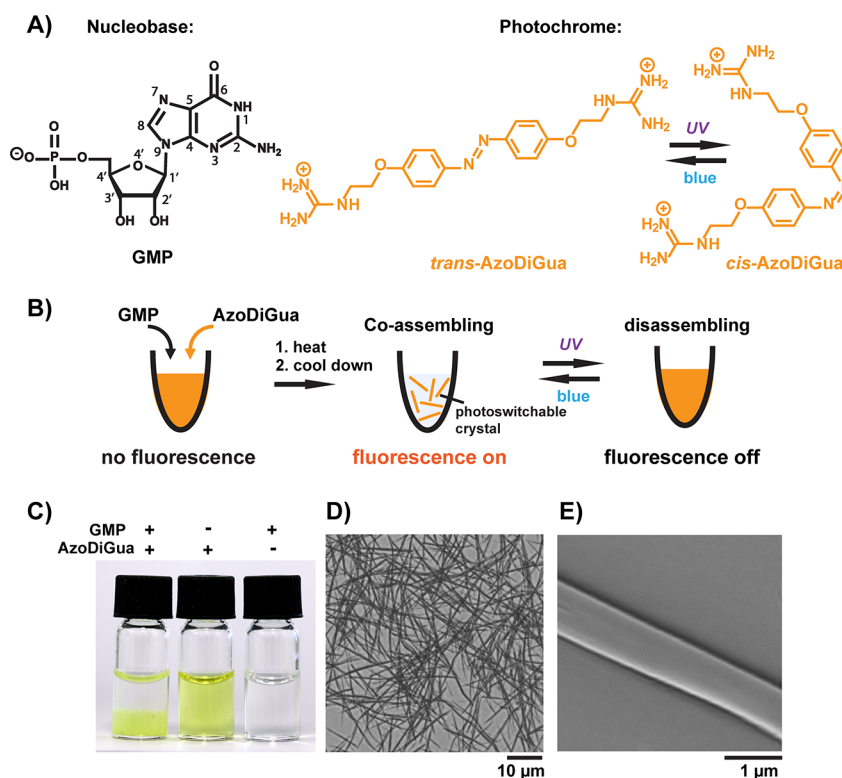


Figure 1. Building a fluorescent, photoswitchable crystal by coassembly of a nucleobase and a photochromic intercalator. (A) Molecular structures of the nucleobase, guanosine monophosphate (GMP), and the photochrome, a symmetric azobenzene diguanidinium compound (AzoDiGua), used in this study. (B) GMP (5 mM) and AzoDiGua (0.2 mM) were mixed in acetic acid buffer (10 mM in water, pH = 3.8), heated to 90 °C, and slowly cooled to 4 °C to form photoswitchable fluorescent crystals. After assembly, crystals were characterized and manipulated at room temperature (RT). (C) Photographs of solutions prepared by different combinations of GMP and AzoDiGua, 20 min at RT after the assembly process. (D,E) Transmission optical (D) and scanning electron (E) microscopy images of the resulting crystals deposited on glass after drop-casting and water evaporation.

building bricks. By exploiting the natural self-arrangement characteristics of nucleobases, we found that this new way of organizing azobenzenes allowed us to obtain crystals with aggregation-induced fluorescence emission while maintaining a strong and reversible response to light stimulation.

Among nucleobases, guanine represents a particularly interesting component for scaffolding supramolecular organizations. Because of the presence of both self-complementary donor and acceptor sites for hydrogen bonds and aromatic rings favoring π - π stacking, it can self-assemble into multiple hydrogen-bonding structures like G-quartets or quadruplexes,²⁵ showing potential in biosensors, material science, and organic electronics.^{26–28} Efforts have also been made to expand the dynamics of the structure, which resulted in a variety of stimuli-responsive systems, the majority of them being controlled by solution composition (pH, ionic composition). Conversely, external control by a light stimulus has been achieved in much fewer cases and only with G-quartet structures by covalent modification or noncovalent π - π stacking strategies to incorporate a photosensitive moiety.^{29–38} However, all of these light-sensitive structures have consisted of a few repeating units, and neither micrometer-sized nor crystalline materials have been constructed. Here, we describe for the first time light-responsive, highly organized, supramolecular architectures containing guanosine monophosphate (GMP) with a needle-like geometry and a length of around one hundred micrometers. Both structure and light-responsiveness resulted from the coassem-

bly of GMP with a hydrophilic, azobenzene-containing DNA intercalator, called AzoDiGua.³⁹ This process relied on a network of hydrogen bonds and π - π stacking involving both components, resulting in a structure that is different from the G-quartet-based architecture that was reported for most GMP-based systems. In this Article, we describe the protocol for coassembling GMP and AzoDiGua, determine the structure of the resulting crystals, characterize their reversible assembling character in response to pH or light stimulation, and analyze their fluorescence properties. We finally exploit the light-responsiveness of these new assemblies to demonstrate a combination of unique properties, such as photoreversible assembly, optical growth control, light-gated permeability, and photoswitchable fluorescence.

RESULTS AND DISCUSSION

Preparation of the Supramolecular Hybrid Crystals.

Figure 1 shows the concept of our coassembly method to generate hybrid crystals with both fluorescence and light-responsiveness. It consisted of the coassembly of the GMP nucleobase with a photochrome, here an azobenzene-containing symmetric divalent guanidinium compound (AzoDiGua) having photosensitive DNA intercalating properties³⁹ (Figure 1A). GMP (5 mM) and AzoDiGua (0.2 mM) were mixed in acetic acid buffer (10 mM in water, pH = 3.8) at room temperature, heated to 90 °C prior to slowly cooling to 4 °C at a speed of 1 °C/min (Figure 1B). Note that the assembly can be directly done at room temperature, but the crystal

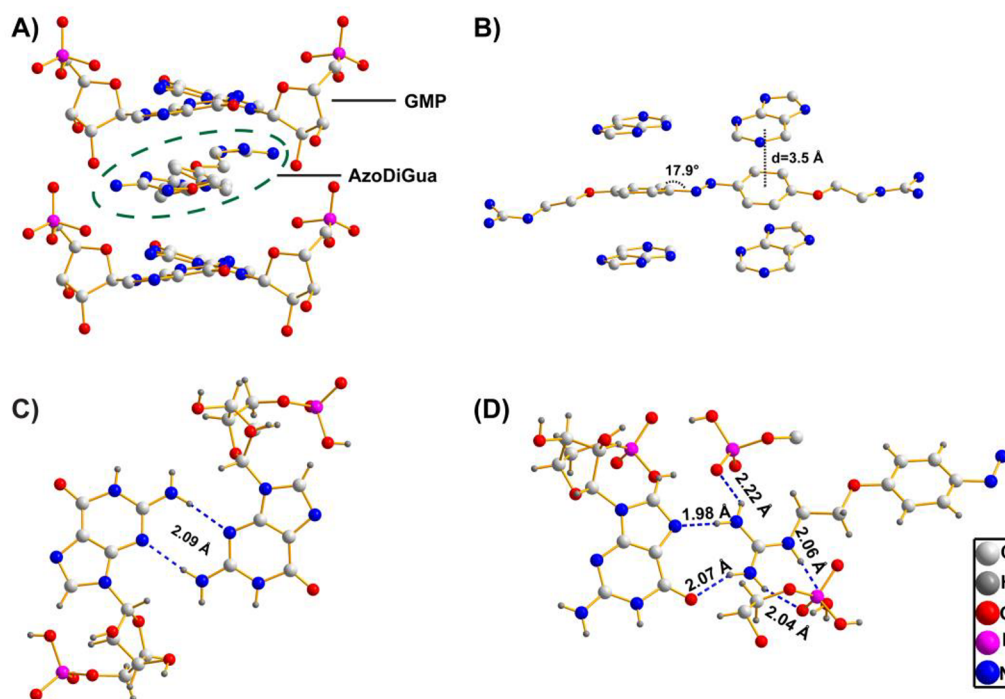


Figure 2. Single-crystal X-ray crystallography reveals the structure of the GMP/AzoDiGua assemblies. (A) Packing diagram of GMP/AzoDiGua crystal. (B) π - π interaction between AzoDiGua and GMP in the crystal. (C) Intermolecular hydrogen bonds between two adjacent GMPs. (D) The guanidinium group of AzoDiGua forms a network of hydrogen bonds with neighboring units. In (A) and (B), hydrogen atoms and functional groups are omitted for clarity. The CIF file is available in SI. Data are deposited at the Cambridge Crystallographic Data Centre (deposition number: CCDC 1563591).

formation is much slower. We have thus used the annealing procedure (heating followed by a slow cooling) throughout this study. After assembly, the suspension was brought back at room temperature (RT), and all experiments were then performed at RT. This process resulted in phase separation occurring only in the presence of both GMP and AzoDiGua (Figure 1C). Optical, electron, and atomic force microscopy observations of the dense phase revealed the presence of well-organized needle-like architectures with an average length and width of 101 ± 46 and 1.9 ± 0.7 μm , respectively (Figures 1D,E and S1). Elementary analysis showed that this solid material was hexahydrated with a stoichiometry AzoDiGua:GMP of 1:2 (Table S1), corresponding to electrostatic neutralization of AzoDiGua by two GMP moieties in their monoanionic form $\text{H}(\text{GMP})^-$ (Figure S2). Increasing pH of the assembling buffer resulted in a progressive deprotonation of $\text{H}(\text{GMP})^-$ (Figure S2) and led to assembled materials with reduced sizes and irregular shapes (Figure S3). Meanwhile, sample prepared at pH 3.8 but with inosine monophosphate (IMP) or adenosine monophosphate (AMP) instead of GMP remained homogeneous (Figure S4). As compared to GMP, IMP lacks the 2-amino group that is typically engaged in one of the three H-bonds of the GC DNA base pair. Similarly, AMP provides one less hydrogen-bond formation site as compared to GMP. All of these observations suggest that both multiple noncovalent hydrogen bonds and electrostatic interactions were involved in the successful coassembly of GMP and AzoDiGua into extended and highly ordered supramolecular structures.

X-ray Structural Analysis. We acquired X-ray diffraction data on a single crystal to gain better insight into the assembled structure and its stabilizing interactions (Figure 2 and Table

S2). Interestingly, although GMP bases were not covalently bound, the relative organization of AzoDiGua and GMP showed similarities with a DNA intercalation motif (Figure 2A,B), emphasizing the interest of using a photosensitive intercalator as one of the two building bricks of the supramolecular structures. There were, however, notable differences from the conventional intercalation mechanism in duplex DNA, which were manifested by the formation of a torsional angle between GMP bases imprinted from the structure of AzoDiGua. Indeed, the analysis showed that the azobenzene moieties in the crystal were in a twisted configuration with a C-C-N=N dihedral angle of 17.9° between the benzene rings and the diazo group, with the two GMP molecules arranged in a nearly parallel manner with respect to the closest benzene plane (Figure 2B). The distance between the centroids of the AzoDiGua benzene rings and the guanine planes was ~ 3.5 Å, which was within the π - π interaction distance.⁴⁰ The arrangement of the molecules also allowed the formation of a network of hydrogen bonds with neighboring units stabilizing the structure (Figures 2C,D and Table S3). The analysis revealed that a pair of guanine bases formed two $\text{NH}_2 \cdots \text{N7}$ hydrogen bonds (2.09 Å, 174.5°), which explains the observed crucial role of the 2-amino group for the ordered structure formation. P-O \cdots H-O hydrogen bonds (1.76 Å, 159.5°) were also found between the phosphate groups of adjacent GMPs (Figure S5), which explains the importance of pH as the monoprotonation of the phosphate group was necessary for assembly to occur. Moreover, the guanidinium group of AzoDiGua not only helped to reduce the repulsion of charged phosphate groups, but also contributed to the assembly through the formation of a network of hydrogen bonds with lengths measured to be within the range 1.92–2.22

Å (Figure 2D). All of these results show the crucial roles of the two components in the self-assembly process leading to the observed crystalline structure: both AzoDiGua and GMP synergistically participated through the cooperative action of electrostatics, π - π interactions, and hydrogen-bond network formation.

pH-Responsiveness of the Crystals. We analyzed how the produced self-assembled crystals could be reversibly affected by the application of different stimuli targeting the noncovalent interactions involved in their structure. First, increasing the pH of a solution containing crystals to pH = 8.5 resulted in their rapid dissolution (Figure 3A), due to the

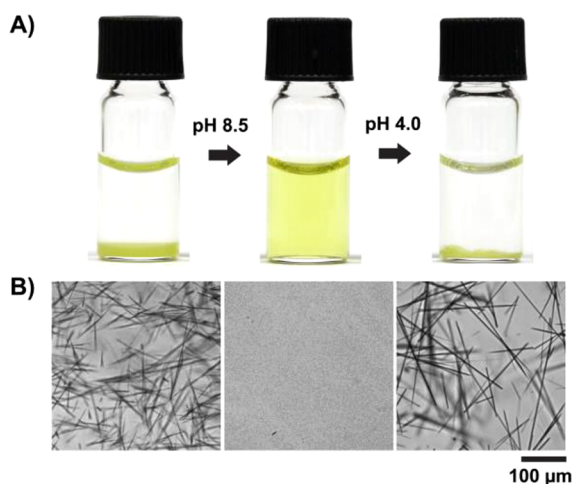


Figure 3. Hybrid crystals are pH-responsive. Photograph of the suspension (A) and in situ transmission optical microscopy images (B) before (left) and after successive addition of NaOH (middle) and HCl (right) at RT. The pH of the solution was 3.8, 8.5, and 4.0, respectively.

deprotonation of GMP and subsequent ruptures of the related hydrogen bonds. Interestingly, when the same solution was brought back to pH = 4, the sample underwent phase separation again. The reassembled material displayed needle-like geometries of size and shape similar to that of the initial crystals (Figure 3B), demonstrating that the coassembled AzoDiGua-GMP supramolecular structure was reversibly addressable through a straightforward pH stimulus.

Photoreversible Crystal Formation/Dissolution. We fixed the pH of the sample suspension (pH = 3.8) and studied the effect of light on the coassembled crystals (Figure 4). Irradiation by UV light (365 nm) at RT resulted in the total dissolution of the crystals in a few minutes (Figure 4A, movie S1), while subsequent blue irradiation (440 nm) of the same solution resulted in the reformation of needle-like crystals (Figure 4A, movie S2). A close-up analysis of the UV-induced dissolution process showed that it started by a bending of the structure prior to breaking and disappearance (Figure 4B). A representative plot of the length of a single crystal versus time showed two-step dissolution kinetics composed of a first slow process followed by a much faster one (Figure 4C, movie S3). When green irradiation (535 nm) where AzoDiGua does not absorb was used instead of UV, neither the dissolution process nor any morphology transformation of the crystal was detected. We thus conclude that the disassembling process comes from the photoisomerization of AzoDiGua from *trans* to *cis* isomer upon UV irradiation.³⁹ The UV-induced bending of

the crystal at the early stage of irradiation was attributed to anisotropic exposure to the UV stimulus leading to uneven *trans*–*cis* AzoDiGua photoisomerization features at the surface of the crystals. This speculation was supported by observing the recovery of a straight needle by applying blue irradiation (30 s) after a very short UV pulse (0.5 s), that is, as soon as the crystal started to bend (Figure S6). After the process was repeated twice, a defect was observed on the crystal surface, indicating a preferential location on the crystal surface for the dissolution to start. To know whether the formation of *cis*-AzoDiGua upon UV irradiation was occurring only at the crystal surface or also in its core, we irradiated a crystal suspension by a moderate UV irradiation (4 min) so that the photosensitive crystals were only partially dissolved. The suspension was centrifuged immediately after UV irradiation, and we compared by absorption spectroscopy the composition of the supernatant to that of the pellet redissolved in water (Figure S7). Clearly, the pellet, and thus the remaining crystal structures after UV, were composed of *trans*-AzoDiGua, while *cis*-AzoDiGua was detected in the supernatant only, that is, in the surrounding medium of the irradiated crystals. We can thus propose the following UV-induced crystal dissolution process. UV irradiation induced the *trans*–*cis* isomerization of AzoDiGua molecules present on the surface of the crystals, which disrupted the local π - π and hydrogen-bond interaction network. The *cis*-AzoDiGua molecules disengaged from the surface and diffused into the bulk as a result of their hydrophilicity. This led to the exposure of a fresh crystal surface to the light, and the disassembly process continued until the full dissolution of the crystal. This suggested diffusion-limited mechanism explains why the full crystal dissolution required significantly more time than that for AzoDiGua to reach the photostationary state in solution under UV irradiation.³⁹ Blue irradiation after such UV-induced dissolution was shown to trigger a recrystallization process (Figure 4A, movie S2). The reassembled material displayed needle-like structures similar to those before UV irradiation, but with a length typically 30% longer (Figure 4E). The needle length distribution (Figure S8) showed an increase from 101 ± 46 to 136 ± 30 μm (mean \pm sd, $n = 112$ and $n = 100$, respectively), which was found to be statistically significant (t test: p -value = 1.5×10^{-10}). Figure 4B, bottom depicts the track of a representative single structure, which elongated from both ends with increased time, with an estimated initial growth speed of around $0.4 \mu\text{m s}^{-1}$ (Figure 4D, movie S3). Because AzoDiGua was shown to be rapidly converted into a *trans*-rich photostationary state upon blue irradiation,³⁹ we propose the following mechanism of blue-induced recrystallization. After UV-irradiation, the photostationary *cis*-rich state contained a small fraction of *trans*-AzoDiGua molecules, which were probably engaged in *trans*-AzoDiGua-GMP clusters that were too small to be detected by optical microscopy. Blue irradiation strongly enriched the solution into *trans*-AzoDiGua molecules that progressively either coassembled on preformed structures or nucleated new ones. The presence of *trans*-AzoDiGua-GMP clusters after UV irradiation might thus act as nuclei and explain the formation, after blue irradiation, of crystals that were larger and in a smaller number than before the UV irradiation step (Figure S8). All of these results show that the photoisomerization properties of AzoDiGua were successfully preserved in the self-assembled structures to generate 100 μm -long azobenzene-GMP crystals with photo-reversible assembly capability.

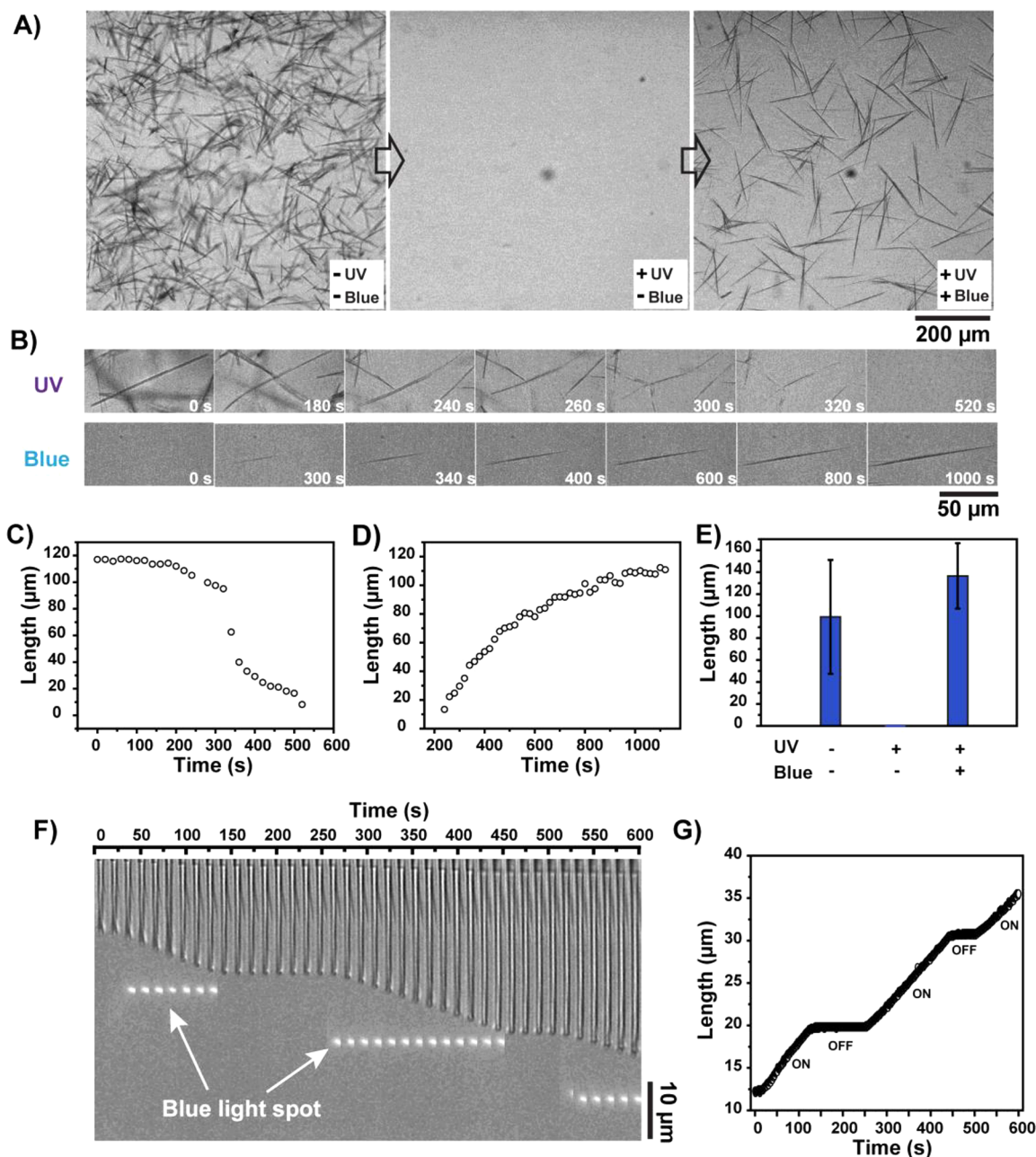


Figure 4. Reversible photocontrol of crystallization. (A–E) In situ, real-time transmission optical microscopy characterization of a suspension of crystals before (–UV, –blue) and after successive irradiation by UV (365 nm, 2.3 mW cm^{-2}) for 10 min (+UV, –blue), and by blue (440 nm, 16 mW cm^{-2}) for 5 min (+UV, +blue). Wide-field representative images in a given irradiated area (A). Time lapse observation and corresponding crystal length of the UV-induced dissolution (B top, C) and of the blue-induced recrystallization (B bottom, D) of a single crystal. Average crystal length (mean \pm sd on ≥ 100 crystals) for the successive irradiation conditions (E). (F,G) High-magnification transmission optical microscopy observation of the recrystallization of a single crystal guided by a blue light spot (488 nm, spot size $1.6 \mu\text{m}$) in a solution previously irradiated by a larger UV light spot (365 nm, spot size $412 \mu\text{m}$) to locally dissolve crystals in the irradiated area. The blue spot irradiation zone was made visible by the fluorescence emission of fluorescein added to the buffer (1 nM). Kymograph of the crystal growth (F). Length of the crystal versus time (G).

Dynamic Photocontrol of a Single-Crystal Growth. In materials science, controlling the kinetics of material growth until desired dimensions, once the parameters like temperature and concentration are set, is a desirable challenge. We thus explored how the dimension of a single needle-shaped crystal could be controlled in a remote and dynamic way by light (Figure 4F,G, movie S4). To this end, we locally irradiated a crystal suspension using a focused UV beam to fully dissolve the solid material in the irradiated area. A much smaller focused laser spot of blue light then was applied in front of a

selected needle and switched on and off in a dynamic manner. Figure 4F and G shows that the growth of the needle was strictly correlated with the application of the light stimulus. The needle grew at almost constant speed when the light was on, while the growth was momentarily stopped as long as the light was kept off. This unique feature allowed us to dynamically control the growth of the targeted single crystal by light with precise spatiotemporal resolution.

Light-Gated Permeable Material. We then explored how the photoreversible assembly/disassembly properties demon-

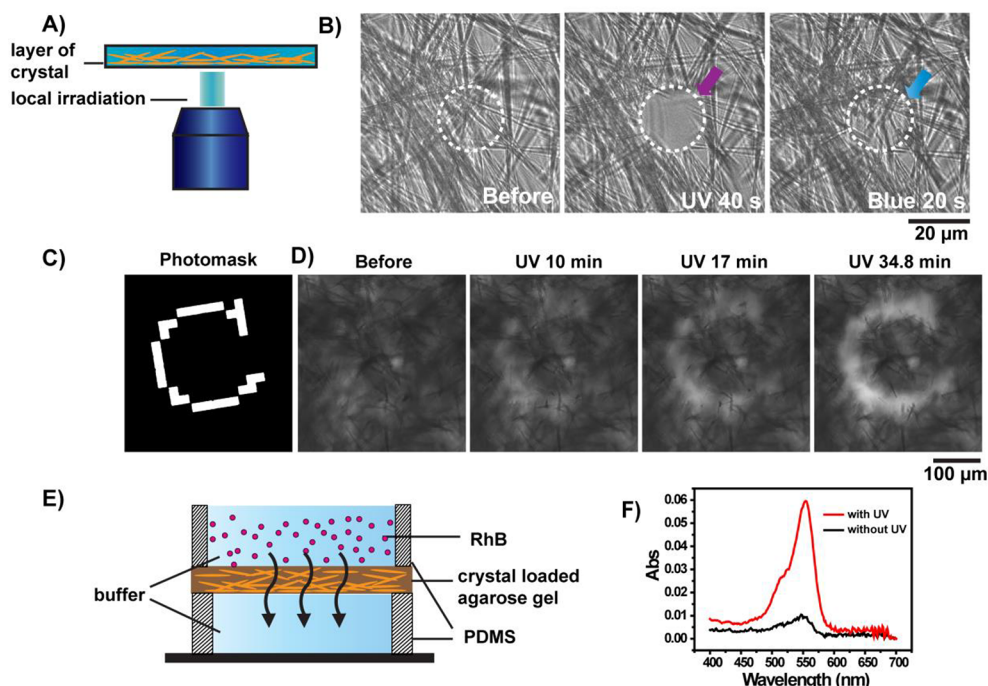


Figure 5. Light-gated permeability in a crystal layer. (A,B) A thin layer of crystals is locally irradiated with a circular spot ($921 \mu\text{m}^2$) inside the suspension buffer (A). In situ transmission microscopy images (B) before (left) and after successive irradiation by UV (365 nm , 4 mW cm^{-2}) for 40 s (middle) and blue (440 nm , 28 mW cm^{-2}) for 20 s (right). The dashed circle indicates the irradiated area. (C,D) A thick layer (approximately $100 \mu\text{m}$) of crystals is locally irradiated by UV through a photomask displaying the letter “C” (C). In situ transmission of the crystal layer a function of irradiation time (D). (E,F) A 0.9 mm thick hybrid membrane composed of crystals embedded in agarose gel is placed between two polydimethylsiloxane (PDMS) compartments. The upper (8 mm diameter) and the lower (3 mm diameter) compartments contain GMP (4.6 mM) in acetic acid buffer (10 mM in water, $\text{pH} = 3.8$), while Rhodamine B (RhB, 0.1 mM) is supplemented only in the upper one (E). Absorption of the solution in the bottom compartment 20 min after the addition of RhB, with (red curve) or without (black curve) continuous irradiation by UV (365 nm , 11 mW cm^{-2}) (F).

strated on individual crystals could be exploited to control the permeability of extended materials composed of a large number of photoresponsive crystals. We first prepared a thin layer of crystals and found that the successive application of focused UV and blue light allowed us to dynamically open and close a single pore at the lit area (Figure 5A,B, movie S5). The UV-induced pore formation was also successful with a thicker layer ($\sim 100 \mu\text{m}$) but required prolonged irradiation time. Interestingly, the size and shape of the light-induced pore reproduced well the spot dimensions, allowing us to create a hole in the material with an arbitrary, user-defined shape (Figure 5C,D, movie S6). We then embedded the photoresponsive crystals inside a thin layer of agarose gel to form a 0.9 mm thick membrane that we placed, in a sandwich configuration, between two aqueous buffer compartments (Figure 5E). The upper compartment was initially loaded with Rhodamine B dye (RhB), and we measured the absorbance of the lower compartment solution 20 min after loading RhD in the upper chamber. The absorbance spectrum displayed a peak around the absorption maximum of RhB (554 nm) showing that the dye diffused through the membrane. Interestingly, the absorbance was approximately 6 times higher when the membrane was exposed to UV, demonstrating an enhanced permeability of the membrane material upon UV exposure. These simple proof-of-concept demonstrations show that the photoreversible assembly character of the crystals can be easily implemented to design and build materials with user-controlled and light-gated permeability.

Photoswitchable Fluorescence. We also found that the supramolecular AzoDiGua-GMP crystals were fluorescent upon blue excitation (Ex/Em $488/493\text{--}575 \text{ nm}$), allowing us to observe them by fluorescence microscopy (Figure 6A). The crystal material displayed a maximal emission at around 600 nm and a wide excitation range from 350 to 500 nm (Figure 6B). Notably, under the same excitation conditions, the fluorescence emission of the hybrid crystal solution was 58 times stronger than that of AzoDiGua alone (Figure S9). Apart from a much lower intensity, the emission spectrum of AzoDiGua alone displayed features similar to that of the crystal. This shows that the fluorescence properties mainly emerged from the specific supramolecular organization of AzoDiGua within the coassembled crystal. As compared to AzoDiGua alone, the absorption of AzoDiGua in the crystal displayed a red-shift attributed to the $\pi\text{--}\pi$ and hydrogen-bond interaction (Figure S10). The absorption band that associated with the $\pi\text{--}\pi^*$ ($S_2 \leftarrow S_0$) transition of the azobenzene unit shifted from 357 to 370 nm . Meanwhile, a new strong shoulder band appeared at around 470 nm , where the forbidden $n\text{--}\pi^*$ ($S_1 \leftarrow S_0$) transition of the *trans* isomer is located. We attribute the observed fluorescence in needle crystals to a relaxation mechanism of the S_1 excited state in the cocrystalline state that is different from that of AzoDiGua alone in solution. Crystallography data showed a restricted conformation of AzoDiGua due to its arrangement with neighboring GMPs, making rotation or inversion relaxation processes upon photoexcitation not favorable. We thus propose that the suppression of the nonradiative relaxation was responsible for

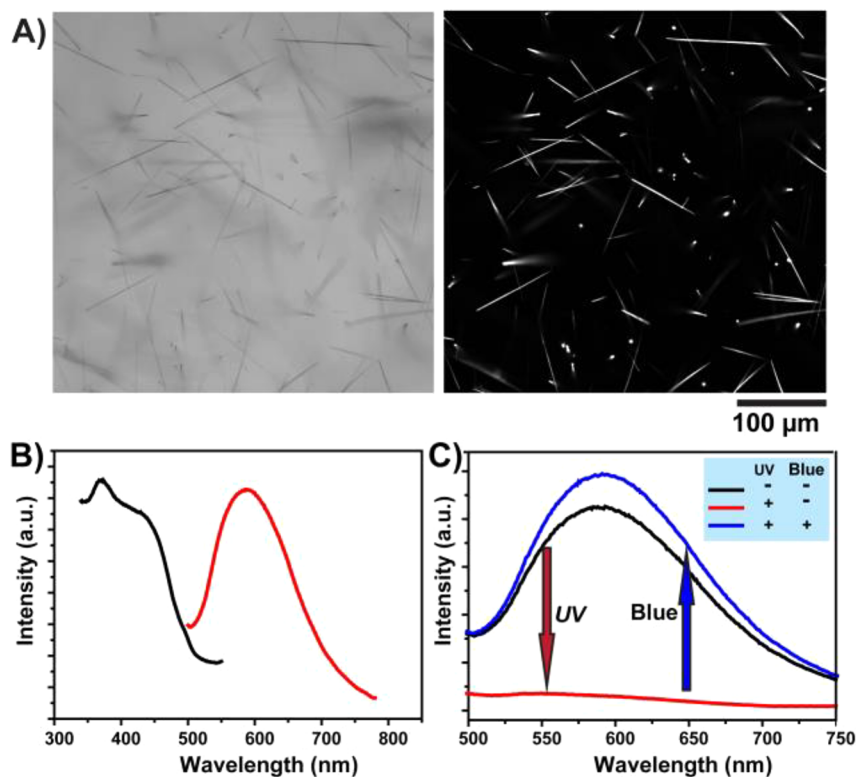


Figure 6. Photoswitchable fluorescent crystals. (A) Transmission (left) and confocal fluorescence (right, 488/493–575 nm) images of crystals in the suspension buffer. (B) Fluorescence excitation (at 597 nm emission, black curve) and emission (at 400 nm excitation, red curve) spectra of the crystal suspension. (C) Fluorescence emission spectrum (excitation 410 nm) of a crystal suspension (200 μL , 0.6 g L^{-1}) before (black curve) and after successive irradiation by UV (365 nm, 11 mW cm^{-2}) for 25 min (red curve) and blue (440 nm, 16 mW cm^{-2}) for 10 min (blue curve).

the greatly enhanced fluorescence emission. Similar effects have been regularly reported in azobenzene crystals, but all fluorescent crystalline systems reported so far lost most of their photoisomerization ability upon crystallization. Here, the unique supramolecular nature of the coassembled AzoDiGua-GMP crystals allowed us to maintain their photoswitching characteristics (Figures 4 and 5). We thus exploited the combination of the photoreversible assembly with the crystallization-induced fluorescence to analyze how fluorescence could be modulated by light in our system. Interestingly, applying UV on a crystal suspension allowed us to switch off the fluorescence, while subsequent blue irradiation on the same solution induced a remarkable recovery of the fluorescence (Figure 6C).

CONCLUSION

We have proposed a new concept of supramolecular assembly associating a nucleobase, here GMP, with an azobenzene-containing photosensitive DNA intercalator called AzoDiGua. This strategy allowed us to obtain properties that could not be achieved by conventional assembly of the same family of compounds taken separately. For instance, we obtained the first 100 μm long GMP-based crystals, while conventional photoresponsive guanine assemblies involving G-quartets or quadruplexes have been mainly limited to small noncrystalline structures of a few repeating units. Similarly, this coassembly principle allowed us to build a new family of azobenzene crystals combining for the first time fluorescence and photoswitchability. Held by a synergic network of π – π , electrostatic, and hydrogen-bond interactions, the resulting crystals presented a combination of unique properties such as

photoreversible assembly, optical shapability, and photo-switchable fluorescence, and could be integrated in membrane-like materials to achieve interesting functionality such as light-gated permeability. We believe that this concept can be easily extended to other molecular bricks carrying additional functionality, thus constituting a promising framework for the facile preparation of a variety of user-defined, stimuli-responsive, and multifunctional self-assembled materials.

ASSOCIATED CONTENT

Supporting Information

The Supporting Information is available free of charge on the ACS Publications website at DOI: 10.1021/jacs.9b02836.

Material and methods; Figures S1–S11; Tables S1 and S2; crystal characterization; effect of pH and nucleotide nature on assembling; single-crystal X-ray analysis; crystal photo-responses; crystal fluorescence properties; and morphology of crystal-loaded hybrid agarose gel (PDF)

Transmission microscopy observation of crystal melting triggered by UV (AVI)

Transmission microscopy observation of the re-assembling of GMP and AzoDiGua under blue light (AVI)

Transmission microscopy observation of crystal melting triggered by UV, followed by recrystallization triggered by blue (AVI)

Transmission microscopy observation of single crystal grown under control of a 488 nm laser spot (AVI)

Transmission microscopy observation of a pore in a thin crystal layer, opened by UV irradiation and closed back after blue exposure (AVI)

Transmission microscopy observation of the formation of a C-shaped pore in a thick crystal layer by UV irradiation through a photomask (AVI)

X-ray crystallographic information for the AzoDiGua/GMP crystal structure (CIF)

AUTHOR INFORMATION

Corresponding Author

*damien.baigl@ens.fr

ORCID

Sergii Rudiuk: 0000-0003-1728-1163

Damien Baigl: 0000-0003-1772-3080

Present Address

[§]Key Laboratory for Water Quality and Conservation of the Pearl River Delta, Ministry of Education, Institute of Environmental Research at Greater Bay, Guangzhou University, Guangzhou 510006, China.

Notes

The authors declare no competing financial interest.

ACKNOWLEDGMENTS

This work was supported by the European Research Council (ERC) [European Community's Seventh Framework Programme (FP7/2007-2013)/ERC Grant Agreement no. 258782] and by the "PSL-Chimie" program. We thank Y. Chen for providing access to his SEM apparatus.

REFERENCES

- (1) Russew, M.-M.; Hecht, S. Photoswitches: From Molecules to Materials. *Adv. Mater.* **2010**, *22* (31), 3348–3360.
- (2) Brieke, C.; Rohrbach, F.; Gottschalk, A.; Mayer, G.; Heckel, A. Light-Controlled Tools. *Angew. Chem., Int. Ed.* **2012**, *51*, 8446–8476.
- (3) Baigl, D. Photo-Actuation of Liquids for Light-Driven Microfluidics: State of the Art and Perspectives. *Lab Chip* **2012**, *12* (19), 3637–3653.
- (4) Fliegl, H.; Köhn, A.; Hättig, C.; Ahlrichs, R. Ab Initio Calculation of the Vibrational and Electronic Spectra of Trans - and Cis -Azobenzene. *J. Am. Chem. Soc.* **2003**, *125* (32), 9821–9827.
- (5) Kassem, S.; van Leeuwen, T.; Lubbe, A. S.; Wilson, M. R.; Feringa, B. L.; Leigh, D. A. Artificial Molecular Motors. *Chem. Soc. Rev.* **2017**, *46* (9), 2592–2621.
- (6) Beharry, A. A.; Woolley, G. A. Azobenzene Photoswitches for Biomolecules. *Chem. Soc. Rev.* **2011**, *40* (8), 4422–4437.
- (7) Matharu, A. S.; Jeeva, S.; Ramanujam, P. S. Liquid Crystals for Holographic Optical Data Storage. *Chem. Soc. Rev.* **2007**, *36* (12), 1868.
- (8) Lubbe, A. S.; Szymanski, W.; Feringa, B. L. Recent Developments in Reversible Photoregulation of Oligonucleotide Structure and Function. *Chem. Soc. Rev.* **2017**, *46* (4), 1052–1079.
- (9) Diguët, A.; Guillermic, R. M.; Magome, N.; Saint-Jalmes, A.; Chen, Y.; Yoshikawa, K.; Baigl, D. Photomanipulation of a Droplet by the Chromocapillary Effect. *Angew. Chem., Int. Ed.* **2009**, *48* (49), 9281–9284.
- (10) Estévez-Torres, A.; Crozatier, C.; Diguët, A.; Hara, T.; Saito, H.; Yoshikawa, K.; Baigl, D. Sequence-Independent and Reversible Photocontrol of Transcription/Expression Systems Using a Photo-sensitive Nucleic Acid Binder. *Proc. Natl. Acad. Sci. U. S. A.* **2009**, *106* (30), 12219–12223.
- (11) Venancio-Marques, A.; Barbaud, F.; Baigl, D. Microfluidic Mixing Triggered by an External LED Illumination. *J. Am. Chem. Soc.* **2013**, *135*, 3218–3223.
- (12) Bisle, H.; Rau, H. Fluorescence of Noncyclic Azo Compounds with a Low-Lying $1(n,\pi^*)$ State. *Chem. Phys. Lett.* **1975**, *31* (2), 264–266.
- (13) Yoshino, J.; Furuta, A.; Kambe, T.; Itoi, H.; Kano, N.; Kawashima, T.; Ito, Y.; Asashima, M. Intensely Fluorescent Azobenzenes: Synthesis, Crystal Structures, Effects of Substituents, and Application to Fluorescent Vital Stain. *Chem. - Eur. J.* **2010**, *16* (17), 5026–5035.
- (14) Shimomura, M.; Kunitake, T. Fluorescence and Photoisomerization of Azobenzene-Containing Bilayer Membranes. *J. Am. Chem. Soc.* **1987**, *109* (17), 5175–5183.
- (15) Tsuda, K.; Dol; Gensch, T.; Hofkens, J.; Latterini, L.; Weener; Meijer; De Schryver. Fluorescence from Azobenzene Functionalized Poly(Propylene Imine) Dendrimers in Self-Assembled Supramolecular Structures. *J. Am. Chem. Soc.* **2000**, *122* (14), 3445–3452.
- (16) Han, M.; Hara, M. Intense Fluorescence from Light-Driven Self-Assembled Aggregates of Nonionic Azobenzene Derivative. *J. Am. Chem. Soc.* **2005**, *127* (31), 10951–10955.
- (17) Han, M. R.; Hirayama, Y.; Hara, M. Fluorescence Enhancement from Self-Assembled Aggregates: Substituent Effects on Self-Assembly of Azobenzenes. *Chem. Mater.* **2006**, *18* (12), 2784–2786.
- (18) Tsai, B.-K.; Chen, C.-H.; Hung, C.-H.; Hsiao, V. K. S.; Chu, C.-C. Photoswitchable Fluorescence on/off Behavior between Cis- and Trans-Rich Azobenzenes. *J. Mater. Chem.* **2012**, *22* (39), 20874.
- (19) Ren, H.; Chen, D.; Shi, Y.; Yu, H.; Fu, Z. A Carboxylic Azo Monomer and Its Homopolymer: Synthesis, Self-Organization and Fluorescence Behaviour in Solution. *Polym. Chem.* **2015**, *6* (2), 270–277.
- (20) Jee, A.-Y.; Lee, Y.; Lee, M.; Kim, M. H. Communication: Time-Resolved Fluorescence of Highly Single Crystalline Molecular Wires of Azobenzene. *J. Chem. Phys.* **2012**, *136* (12), 121104.
- (21) Han, M.; Cho, S. J.; Norikane, Y.; Shimizu, M.; Kimura, A.; Tamagawa, T.; Seki, T. Multistimuli-Responsive Azobenzene Nanofibers with Aggregation-Induced Emission Enhancement Characteristics. *Chem. Commun.* **2014**, *50* (99), 15815–15818.
- (22) Han, M.; Takeoka, Y.; Seki, T. Facile Morphological Control of Fluorescent Nano/Microstructures via Self-Assembly and Phase Separation of Trigonal Azobenzenes Showing Aggregation-Induced Emission Enhancement in Polymer Matrices. *J. Mater. Chem. C* **2015**, *3* (16), 4093–4098.
- (23) Lee, S.; Oh, S.; Lee, J.; Malpani, Y.; Jung, Y.-S.; Kang, B.; Lee, J. Y.; Ozasa, K.; Isoshima, T.; Lee, S. Y.; et al. Stimulus-Responsive Azobenzene Supramolecules: Fibers, Gels, and Hollow Spheres. *Langmuir* **2013**, *29* (19), 5869–5877.
- (24) Han, M.; Cho, S. J.; Norikane, Y.; Shimizu, M.; Seki, T. Assembly of an Achiral Chromophore into Light-Responsive Helical Nanostructures in the Absence of Chiral Components. *Chem. - Eur. J.* **2016**, *22* (12), 3971–3975.
- (25) Gellert, M.; Lipsett, M. N.; Davies, D. R. Helix Formation by Guanylic Acid. *Proc. Natl. Acad. Sci. U. S. A.* **1962**, *48* (12), 2013–2018.
- (26) Davis, J. T. G-Quartets 40 Years Later: From 5'-GMP to Molecular Biology and Supramolecular Chemistry. *Angew. Chem., Int. Ed.* **2004**, *43* (6), 668–698.
- (27) Berger, O.; Adler-Abramovich, L.; Levy-Sakin, M.; Grunwald, A.; Liebes-Peer, Y.; Bachar, M.; Buzhansky, L.; Mossou, E.; Forsyth, V. T.; Schwartz, T.; et al. Light-Emitting Self-Assembled Peptide Nucleic Acids Exhibit Both Stacking Interactions and Watson–Crick Base Pairing. *Nat. Nanotechnol.* **2015**, *10* (4), 353–360.
- (28) Pu, F.; Wu, L.; Ran, X.; Ren, J.; Qu, X. G-Quartet-Based Nanostructure for Mimicking Light-Harvesting Antenna. *Angew. Chem., Int. Ed.* **2015**, *54* (3), 892–896.
- (29) Mayer, G.; Kröck, L.; Mikat, V.; Engeser, M.; Heckel, A. Light-Induced Formation of G-Quadruplex DNA Secondary Structures. *ChemBioChem* **2005**, *6* (11), 1966–1970.
- (30) Heckel, A.; Buff, M. C. R.; Raddatz, M.-S. L.; Müller, J.; Pöttsch, B.; Mayer, G. An Anticoagulant with Light-Triggered Antidote Activity. *Angew. Chem., Int. Ed.* **2006**, *45* (40), 6748–6750.
- (31) Kim, Y.; Phillips, J. A.; Liu, H.; Kang, H.; Tan, W. Using Photons to Manipulate Enzyme Inhibition by an Azobenzene-Modified Nucleic Acid Probe. *Proc. Natl. Acad. Sci. U. S. A.* **2009**, *106* (16), 6489–6494.

- (32) Ogasawara, S.; Maeda, M. Reversible Photoswitching of a G-Quadruplex. *Angew. Chem., Int. Ed.* **2009**, *48* (36), 6671–6674.
- (33) Lena, S.; Neviani, P.; Masiero, S.; Pieraccini, S.; Spada, G. P. Triggering of Guanosine Self-Assembly by Light. *Angew. Chem., Int. Ed.* **2010**, *49* (21), 3657–3660.
- (34) Wang, X.; Huang, J.; Zhou, Y.; Yan, S.; Weng, X.; Wu, X.; Deng, M.; Zhou, X. Conformational Switching of G-Quadruplex DNA by Photoregulation. *Angew. Chem., Int. Ed.* **2010**, *49* (31), 5305–5309.
- (35) Schmidt, T. L.; Koeppel, M. B.; Thevarpadam, J.; Gonçalves, D. P. N.; Heckel, A. A Light Trigger for DNA Nanotechnology. *Small* **2011**, *7* (15), 2163–2167.
- (36) Rivera, J. M.; Silva-Brenes, D. A Photoresponsive Supramolecular G-Quadruplex. *Org. Lett.* **2013**, *15* (10), 2350–2353.
- (37) Thevarpadam, J.; Bessi, I.; Binas, O.; Gonçalves, D. P. N.; Slavov, C.; Jonker, H. R. A.; Richter, C.; Wachtveitl, J.; Schwalbe, H.; Heckel, A. Photoresponsive Formation of an Intermolecular Minimal G-Quadruplex Motif. *Angew. Chem., Int. Ed.* **2016**, *55* (8), 2738–2742.
- (38) Tian, T.; Song, Y.; Wang, J.; Fu, B.; He, Z.; Xu, X.; Li, A.; Zhou, X.; Wang, S.; Zhou, X. Small-Molecule-Triggered and Light-Controlled Reversible Regulation of Enzymatic Activity. *J. Am. Chem. Soc.* **2016**, *138* (3), 955–961.
- (39) Bergen, A.; Rudiuk, S.; Morel, M.; Le Saux, T.; Ihmels, H.; Baigl, D. Photodependent Melting of Unmodified DNA Using a Photosensitive Intercalator: A New and Generic Tool for Photo-reversible Assembly of DNA Nanostructures at Constant Temperature. *Nano Lett.* **2016**, *16* (1), 773–780.
- (40) Janiak, C. A. Critical Account on π - π Stacking in Metal Complexes with Aromatic Nitrogen-Containing Ligands. *J. Chem. Soc. Dalt. Trans.* **2000**, *21*, 3885–3896.